Journal of Inflammation Research Dovepress

Open Access Full Text Article ORIGINAL RESEARCH

Uncovering SPP1$^+$ Macrophage, Neutrophils and Their Related Diagnostic Biomarkers in Intracranial Aneurysm and Subarachnoid Hemorrhage

Haipeng Jie[1,2], Boyang Wang[1,2], Jingjing Zhang[1,2], Xinzhao Wang[3,4], Xiang Song[3], Fan Yang[5], Changning Fu[6], Bo Dong[1,2], Feng Yan[7]

[1]Department of Cardiology, Shandong Provincial Hospital, Cheeloo College of Medicine, Shandong University, Jinan, People's Republic of China; [2]Department of Cardiology, Shandong Provincial Hospital Affiliated to Shandong First Medical University, Jinan, People's Republic of China; [3]Breast Cancer Center, Shandong Cancer Hospital and Institute, Shandong First Medical University and Shandong Academy of Medical Sciences, Jinan, People's Republic of China; [4]REMEGEN, LTD, Yantai Economic & Technological Development Area, Yantai, People's Republic of China; [5]Department of Neurosurgery, Shandong Provincial Hospital Affiliated to Shandong First Medical University, Jinan, People's Republic of China; [6]Department of Critical Care Medicine, Shandong Provincial Hospital, Cheeloo College of Medicine, Shandong University, Jinan, People's Republic of China; [7]Department of Emergency Medicine, Qilu Hospital, Cheeloo College of Medicine, Shandong University, Jinan, People's Republic of China

Correspondence: Feng Yan, Department of Emergency Medicine, Qilu Hospital, Cheeloo College of Medicine, Shandong University, 107 Wenhua West Road, Lixia District, Jinan, 250012, People's Republic of China, Tel +86 18560083857, Email yanfeng@sdu.edu.cn; Bo Dong, Department of Cardiology, Shandong Provincial Hospital, Cheeloo College of Medicine, Shandong University, No. 324, Jingwu Weiqi Road, Huaiyin District, Jinan, 250021, People's Republic of China, Tel +86 13356691808, Email bodong@sdu.edu.cn

Background: Intracranial aneurysms (IA) frequently cause subarachnoid hemorrhage (SAH) and have poor prognosis. However, the molecular mechanisms and diagnostic biomarkers associated with IA and ruptured IA (rIA) remain poorly understood.

Methods: In this study, single-cell and transcriptome datasets were obtained from the GEO database. The cell populations were annotated to identify potential pathogenic subpopulations, followed by intercellular communication, pseudotime, and SCENIC analyses. Proteome-wide and transcriptome-wide Mendelian randomization (MR) analyses were conducted to identify risk factors for IA and SAH. The major pathological changes and diagnostic biomarkers of IA and SAH were identified based on the transcriptome datasets. A clinical cohort was established to identify the diagnostic biomarkers and validate the results.

Results: Macrophages and neutrophils were predominantly increased in IA and rIA tissues, and neutrophils were markedly upregulated in the blood of SAH patients. SPP1$^+$ Macrophage was progressively elevated in aneurysms, promoting vascular smooth muscle cell (VSMC) phenotypic transformation and collagen matrix remodeling through the SPP1 and TGF-β pathways. Furthermore, HIF1α regulon was enriched in SPP1$^+$ Macrophage, mediating inflammation and metabolic reprogramming, which contributed to IA progression. Integrated MR analysis identified CD36 as a risk factor for both IA and SAH, and it has been recognized as an effective blood biomarker for SAH. Neutrophils and their related indicators have emerged as excellent biomarkers of SAH in clinical cohorts.

Conclusion: This study highlighted the detrimental role of SPP1$^+$ Macrophage in IA and SAH using single-cell sequencing and MR analyses. CD36 was identified as a risk factor for IA and SAH and was also an efficient blood biomarker for SAH. In a clinical cohort, neutrophils and related indicators were valuable for the early diagnosis of SAH.

Keywords: intracranial aneurysm, single-cell sequencing, Mendelian randomization, SPP1$^+$ Macrophage, neutrophils

Introduction

Intracranial aneurysm (IA) is recognized as an abnormal protrusion in the intracranial artery, affecting 3–5% of the population. It is the main cause of non-traumatic subarachnoid hemorrhage (SAH) and is generally associated with hypertension, smoking, and a family history of stroke.[1,2] Currently, it is believed that the inflammatory response of the endothelium caused by wall shear stress leads to macrophage infiltration and vascular smooth muscle cell (VSMC) phenotype transformation. Then they further degrade the internal elastic layer and induce collagen matrix remodeling, resulting in pathological dilation and insufficient vascular wall.[3,4] Although the rate of IA detection has significantly

Received: 30 August 2024
Accepted: 26 October 2024
Published: 9 November 2024

increased with the popularization of MRI and CT, the growth and rupture of IA are not completely related to diameter and time.[1,5] Nowadays, surgical treatment, endovascular treatment, and conservative treatment could be chosen according to the position and diameter of the IA, which have greatly improved the prognosis of patients with IA and SAH.[2,6] However, complications and poor prognosis associated with ruptured IA (rIA) should not be ignored. Therefore, identifying the potential regulatory mechanisms and diagnostic biomarkers for IA and rIA is imperative.

A previous study reveals that endothelium-secreted small molecules containing MCP-1 and VCAM-1 attract inflammatory cells, such as macrophages, neutrophils, and lymphocytes, which could interact with VSMCs and fibroblasts to promote IA formation and rupture.[4,7] However, no drugs are recommended for the specific mechanisms of IA, except for observation and surgery.[5] Genomics, proteomics, transcriptomics, and metabolomics are conducive to the discovery of novel regulatory mechanisms, therapeutic targets, and biomarkers.[8] Single-cell sequencing of $CD8^+CD161^+$cells in the cerebrospinal fluid of patients with aneurysmal SAH identifies that CXCL10 is significantly increased in monocytes, which might contribute to leukocyte recruitment to mediate inflammatory activation.[9,10] Combining single-cell sequencing and spatial transcriptomics reveals that the secretory protein THBS1 is upregulated after SAH, promoting apoptosis of meningeal lymphatic vessels and aggravating neurobehavioral dysfunction.[11] Epidemiological studies indicate a significant increase in the incidence of aneurysmal SAH among postmenopausal women. Furthermore, Mendelian randomization (MR) further confirms that sex hormone-binding globulin is a risk factor for its development.[12] Protein quantitative trait loci (pQTL) and expression quantitative trait loci (eQTL) are genetic variation sites associated with protein or gene expression, which are widely used to explore disease mechanisms and drug targets.[13,14] For instance, eQTL and pQTL genome-wide association study (GWAS) data of immune-related genes have been utilized to explore therapeutic targets in patients with IA, as well as to investigate their expressions across different cell types.[15] GWAS data from large cohorts is also utilized to simulate prospective cohort studies, offering valuable insights into identifying diagnostic biomarkers for IA and SAH. Several inflammatory cytokines are causally associated with IA and SAH and may be validated as effective diagnostic biomarkers in clinical cohorts.[16]

Recent studies have demonstrated that the levels of various chemokines in the cerebrospinal fluid and blood of patients with SAH are significantly elevated, which may be associated with poorer clinical outcomes.[17,18] Among these, elevated serum CCL5 levels on the 7th day after SAH could serve as a biomarker for predicting a favorable prognosis.[18] Systemic inflammation indicators, including systemic immune-inflammation index (SII), neutrophil-to-lymphocyte ratio (NLR), platelet-to-neutrophil ratio (PNR), platelet-to-WBC ratio (PWR), and platelet-to-lymphocyte ratio (PLR), are associated with many diseases and provide novel insights into diagnostic biomarkers for IA.[19,20] However, the biomarkers currently used for diagnosing SAH patients and predicting their prognosis have yet to be validated through multi-center prospective cohort studies.

Although significant progress has been made in previous studies, the underlying regulatory mechanisms in the pathogenesis of IA remain to be discovered. In our study, single-cell sequencing datasets were acquired from the NCBI Gene Expression Omnibus (GEO) database to identify interesting cell populations and their underlying pathogenic mechanisms. Proteome-wide MR, transcriptome-wide MR, and transcriptome sequencing datasets were integrated to explore the causality of proteins or genes of interest. A retrospective cohort comprising 281 normal controls, 282 IA, and 133 SAH participants was constructed to identify risk factors and diagnostic biomarkers. Overall, our study aimed to integrate single-cell and transcriptome sequencing, MR, and a clinical cohort to explore the potential modulatory mechanisms, therapeutic targets, and biomarkers in patients with IA and SAH.

Materials and Methods

Clinical Characteristics of IA and SAH Cohort

Patients with IA and SAH who underwent digital subtraction angiography (DSA) between June 2022 and August 2023 at Shandong Provincial Hospital were enrolled in our study. At the same time, healthy participants from the physical examination center were included in the study. Demographic data, medical history, and laboratory examination results were retrospectively collected and reviewed. The inclusion criteria were: (1) age > 18 years; (2) IA diagnosed via CT, MRI, or DSA; and (3) SAH diagnosed via CT, MRI, or lumbar puncture. Participants with recent infectious diseases,

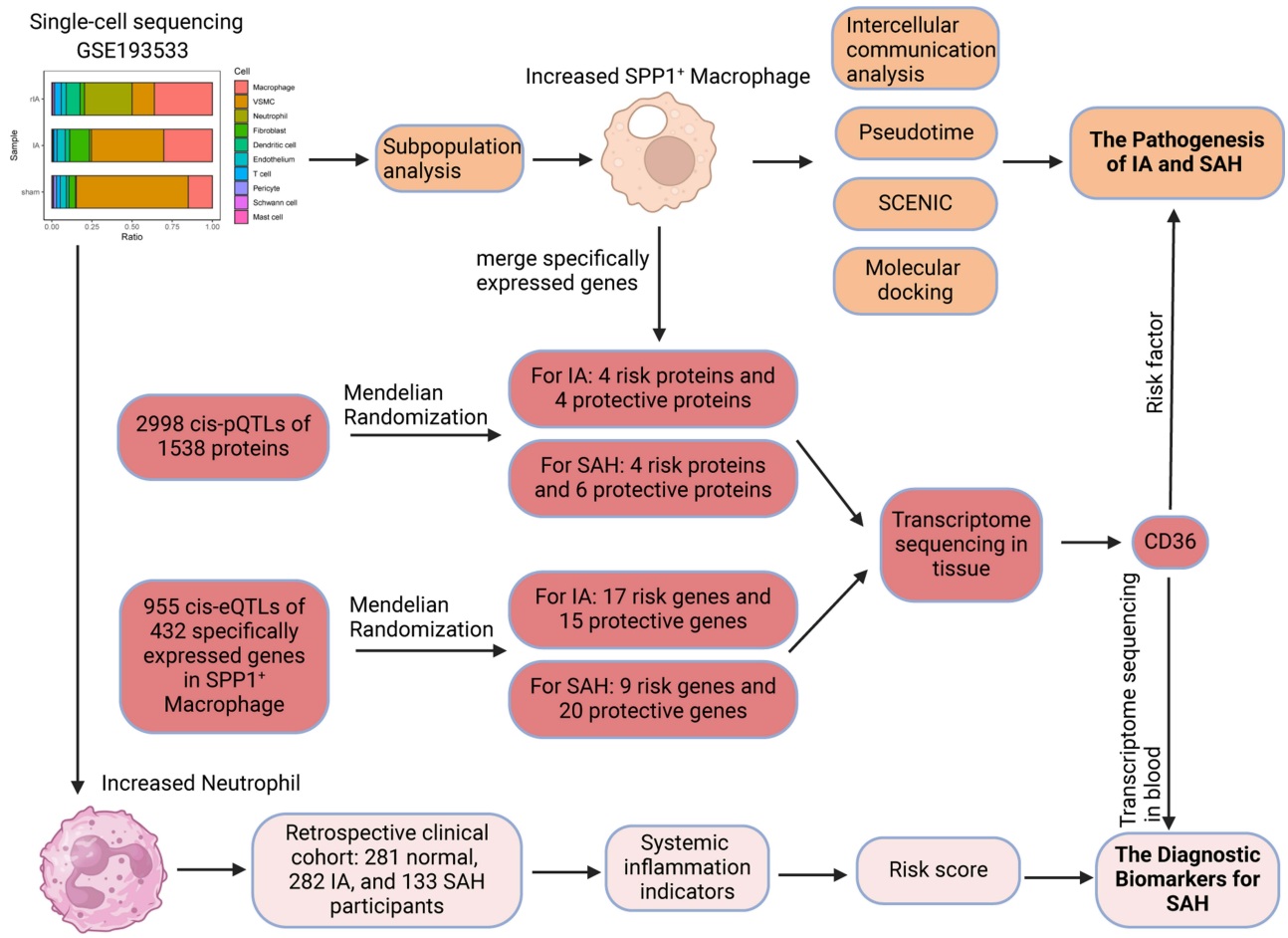

Figure 1 The flow diagram of the study.

acute cerebral infarction, myocardial infarction, autoimmune diseases, SAH caused by other vascular diseases or trauma, or inadequate clinical information were excluded. The Ethics Committee of Shandong Provincial Hospital waived the need for informed consent owing to the retrospective analysis of anonymized data. The researchers ensured that the participants' privacy and rights were safeguarded. The study complied with the principles of the Declaration of Helsinki. Ethics Number: SWYX: NO.2023–535. A flow diagram was presented in Figure 1.

Single-Cell Sequencing Analysis

The single-cell sequencing dataset GSE193533 was acquired from GEO and consisted of 1 sham, IA, and rIA sample.[21] After quality control was completed, the expression matrix of each sample was normalized and log-transformed to calculate the highly variable genes. To remove batch effects, harmony (version 0.1.1) was subsequently utilized to integrate the above expression matrix using the top 3000 highly variable genes. The optimal dimension of 15 and resolution of 0.3 were selected to complete the cell clustering, which was further visualized using Uniform Manifold Approximation and Projection (UMAP). In our study, only cell clusters with correlations ≥ 0.8 were considered to have the possibility of aggregating into one cell population, which was calculated using Spearman's method. CellMarker, SingleR (version 2.0.0), and some known markers were used to annotate the above cell clusters.[22] To evaluate various expressions among cell populations in each group, cell markers or differentially expressed genes (DEGs) were both identified with $|\log FC| \geq 0.25$ and min.pct ≥ 0.1 by performing the Wilcoxon test. Due to the absence of single-cell sequencing data for IA, three AAA mouse models constructed using Angiotensin II, calcium chloride, and elastase were further utilized to validate the results. Detailed information was provided in Supplementary Table 1.

Pseudotime Analysis, Intercellular Communication Analysis, and SCENIC Analysis

Monocle2 (version 2.26.0) predicted the differentiation state of the cell population by learning the changes in gene expression during the process of cell state transition. We adopted the unsupervised clustering method, randomly selected cells with mean expressions > 0.1 and dispersion empirical > 1 * dispersion, to calculate pseudotime and reduce dimensionality with the "DDRTree" algorithm. CellChat (version 1.6.1) predicted the intercellular communication of cell populations based on the expression levels of ligands, receptors, and other cofactor genes. The imported data was used to determine the proportion and interactions of the ligand-receptor pair (L-R pair). Single-cell sequencing not only clarified the roles and fate trajectory of different cells but also constructed a TF regulatory network (named regulon) in which TF and cofactors cooperatively regulated downstream targeted genes using SCENIC (version 1.3.1). The SCENIC analysis was performed according to the standard procedure described by the authors.

Proteome-Wide MR

In the Fenland study conducted by Pietzner et al, the GWAS data of 4,775 proteins from 10,708 participants were tested, identifying 3,323 cis-protein quantitative trait loci (cis-pQTLs).[13] The criteria for cis-pQTLs were defined as follows: (i) achieving genome-wide significance ($p < 5\times10^{-8}$), (ii) removing linkage disequilibrium ($r^2 < 0.001$ in the 10,000kb range), and (iii) strong instrumental variables with an F statistic>10. The GWAS data for IA and SAH were acquired from the FinnGen database, including finn-b-I9_ANEURYSM and finn-b-I9_SAHANEUR. MR was then performed using inverse variance weighted (IVW) for cis-pQTLs corresponding to two or more SNPs, and the Wald ratio method for proteins corresponding to a single SNP. The cis-pQTLs with p-value < 0.05 were excluded through Cochran Q-test and MR-Egger intercept test. Subsequently, the Steiger Direction Test and Steiger Filtering were performed to evaluate their bidirectional causal relationships. Bonferroni correction was not applied in this exploratory study to maximize the identification of potential targets.

Transcriptome-Wide MR

To discover the role of interesting cell subpopulations in IA and SAH, their specific genes were analyzed through Transcriptome-wide MR. The corresponding cis-expression quantitative trait loci (cis-eQTLs) were acquired from the eQTLGen database. The detailed procedure was the same as described above.

The Causality of Collagen Families and Cardiovascular Risk Factors with IA and SAH

Collagen matrix remodeling has been demonstrated to promote the formation and rupture of IA, although the causality remained unclear. Therefore, GWAS data for collagen families was acquired from the IEU database and used to discover causality using the same methods. Similarly, 12 cardiovascular risk factors were identified to explore those associated with IA and SAH.[14] Detailed information was provided in Supplementary Table 2.

Small Molecule Drug Prediction and Molecular Docking

The DGIdb (https://dgidb.org/) database provided drug-gene interactions derived from published articles and databases in a convenient manner. Molecular docking was performed to search for optimal binding patterns using the principles of spatial structural complementarity and energy minimization. Briefly, 3D structures of small-molecule drugs and proteins were acquired from PubChem and PDB, respectively, and were then used to determine the minimal binding energy in AutoDock (version 4.2.6). To visualize the best drug-gene docking model, the predicted model was displayed in a 3D crystal structure using PyMOL (version 2.4.0).

Transcriptome Sequencing Data Analysis

GSE75436, GSE26969, GSE13353, GSE6551, GSE54083, and GSE46337 were processed using the GEOquery or oligo package and were annotated using the corresponding platform files. An average value was selected when multiple probes matched a single gene. Batch effects were further eliminated using the sva package to obtain 24 rIA, 33 IA, and 30 normal samples. Moreover, two blood transcriptome sequencing datasets, GSE36791 and GSE159610, were used to validate the diagnostic biomarkers for IA and SAH, which included 44 SAH, 25 IA, and 43 normal participants. Detailed clinical characteristics were listed (Supplementary Table 3). The limma package was used to identify DEG with |fold change| >1.8 and p-value < 0.05.

Functional Enrichment Analysis and Immune Infiltration Analysis

KEGG enrichment analysis was performed using clusterProfiler package (version 4.9.0.002), and Gene Ontology (GO) enrichment analysis, comprising Molecular Function (MF), Biological Processes (BP), and Cellular Component (CC), was performed using the same methods. Meanwhile, Gene set enrichment analysis (GSEA) was also completed to discover underlying pathways associated with IA and rIA using "c2.cp.v2022.1.Hs.symbols.gmt" from the MSigDB. The CIBERSORT algorithm was then used to detect 22 types of immune cell infiltration in IA and rIA. Based on single-cell sequencing data, deconvolution using CIBERSORT was performed to evaluate cell composition in the transcriptome sequencing data.

Protein-Protein Interaction (PPI) Network and Weighted Gene Co-Expression Network Analysis (WGCNA)

The STRING database (https://string-db.org/) was designed to integrate the associations among proteins confirmed or predicted by experiments or other databases. Cytoscape software (version 3.8.2, http://www.cytoscape.org/) was used to construct the PPI networks. Cytoscape's Molecular Complex Detection (MCODE) plugin was subsequently used to identify and visualize hub modules, which were annotated by enrichment analysis. WGCNA was performed using a scale-free network to cluster genes into various modules, and correlations between modules and clinical characteristics were calculated to identify intriguing modules. In our study, genes in the modules with correlation coefficient ≥ 0.55 were considered as significantly associated with IA and rIA.

Identify Diagnostic Biomarkers and Risk Factors for IA and SAH Based on Transcriptome Sequencing Datasets, MR, and Clinical Cohort

Based on cis-pQTLs and cis-eQTLs from $SPP1^{+}$ Macrophage, three machine-learning algorithms, namely LASSO, Random Forest (RF), and SVM were used to identify diagnostic biomarkers for IA and rIA. These were further validated using blood transcriptome sequencing datasets. Receiver operating characteristic (ROC) curves and area under the curve (AUC) were calculated and visualized. Univariate and multivariate regression analyses were used to identify the risk factors for IA in the clinical cohort. The RF algorithm was used to identify diagnostic biomarkers and risk factors for SAH based on statistically significant variables from the univariate regression analysis. Eventually, the diagnostic biomarkers were integrated into risk score, with diagnostic efficacy visualized using the ROC curve.

Statistical Analysis

The R software (version 4.2.2) was used to analyze the results in our research. Categorical variables were described as percentages and assessed using the chi-square test. Normally distributed continuous variables were evaluated using the Student's t-test and one-way analysis of variance (ANOVA), whereas the Wilcoxon rank-sum test and Kruskal-Wallis test were used for non-normally distributed continuous variables. The correlation coefficient was calculated using Spearman's method. Statistical significance was set at $p < 0.05$.

Results

Cell Population in IA and rIA

After completing quality control, 12,812 cells were obtained from the sham, IA, and rIA groups. These were annotated as 10 cell populations, including macrophages, VSMCs, neutrophils, fibroblasts, dendritic cells, endothelia, T cells, pericytes, Schwann cells, and mast cells (Figure 2A). Macrophages and neutrophils predominantly increased in number as the disease progressed (Figure 2B). In contrast to macrophages, VSMCs gradually decreased. Moreover, necroptosis, apoptosis, and immunogenic cell death were enhanced with the progression of IA (Supplementary Figure 1). Higher chemokine and collagen remodeling scores in IA and rIA indicated immune cell infiltration and collagen remodeling. Meanwhile, the contractile score was also indicative of VSMC phenotypic transformation in IA (Figure 2C–E). The corresponding genes were listed in Supplementary Table 4. The DEGs in the cell populations among the three groups were calculated and visualized (Figure 2F and G). Chemokines, including CCL5 and CXCL10 in macrophages and CXCL2 in endothelia, were upregulated in IA. SPP1 was highly expressed in fibroblasts, VSMCs, endothelia in IA, and macrophages in rIA.

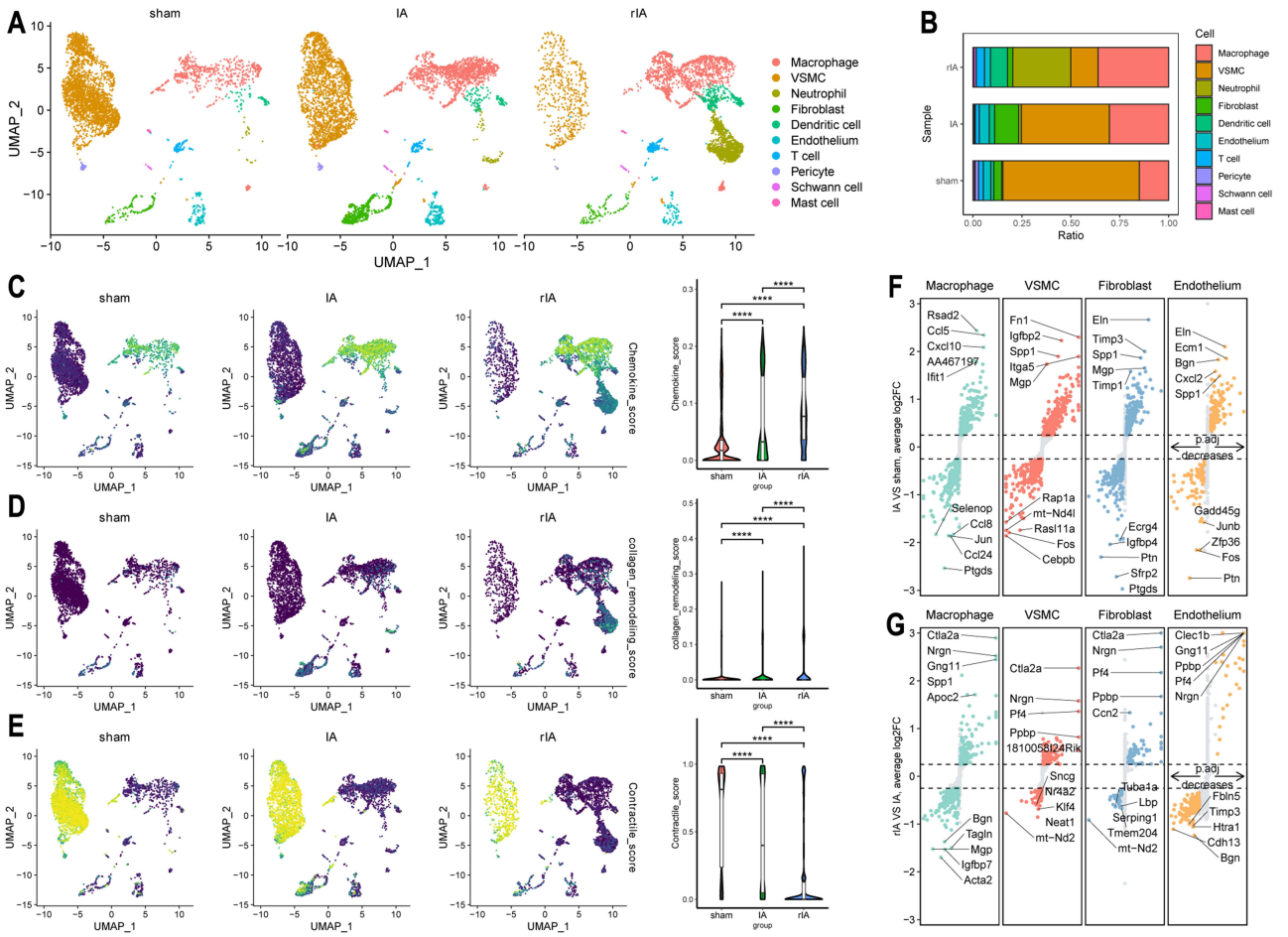

Figure 2 Overview of cell populations in sham, IA, and rIA groups. (**A**) UMAP plots of 10 cell populations in 3 groups. (**B**) UMAP plots of 10 cell populations in 3 groups. (**C–E**) UMAP plots and box plots of Chemokine score, Collagen matrix score, and Contractile score in 3 groups. (**F**) Volcano plots of DEGs in macrophages, VSMCs, fibroblasts, and endothelia in IA. (**G**) Volcano plots of DEGs in macrophages, VSMCs, fibroblasts, and endothelia in rIA. ****p < 0.0001.

Intercellular Communication in IA and rIA

Intercellular communication analysis revealed that almost all intercellular communication increased in IA, especially in VSMCs, fibroblasts, and endothelia (Figure 3A). Although the overall level of intercellular communication decreased in rIA, the interactions of immune cells, such as macrophages, dendritic cells, and neutrophils, were still enhanced (Figure 3B). The SPP1, TGF-β, and CCL pathways were predominantly upregulated in the IA group. The SPP1 pathway was mainly enriched in fibroblasts, VSMCs, and macrophages, and their corresponding L-R pairs were increased in IA (Figure 3C, D and F). Similar results were observed in the TGF-β pathway (Figure 3E). Notably, neutrophils were predominantly increased in rIA, probably promoting the progression of rIA. Almost all L-R pairs of the SPP1 pathway, targeting VSMCs and fibroblasts from neutrophils, were enhanced (Figure 3G). We also found that the PTN, VTN, and MK pathways were significantly down-regulated in the rIA group. TF regulons targeting macrophages, VSMCs, fibroblasts, and endothelia were reduced using t-distributed Stochastic Neighbor Embedding (t-SNE) (Figure 3H and I). Among them, the MAFB regulon was recognized as macrophage-specific (Figure 3J) and was also demonstrated to mediate the transition of monocytes to macrophages.[23] The corresponding TF regulons were selected to identify modulated cell subpopulations (Figure 3K–M).

SPP1^{+} Macrophage Accelerated the Progression of IA Through SPP1 and TGF-β Pathways

Macrophages gradually increased with IA progression, indicating their significant roles. 6 subpopulations were identified to determine the potential modulatory mechanisms (Figure 4A and B). Notably, the M1 subpopulation, which highly expressed

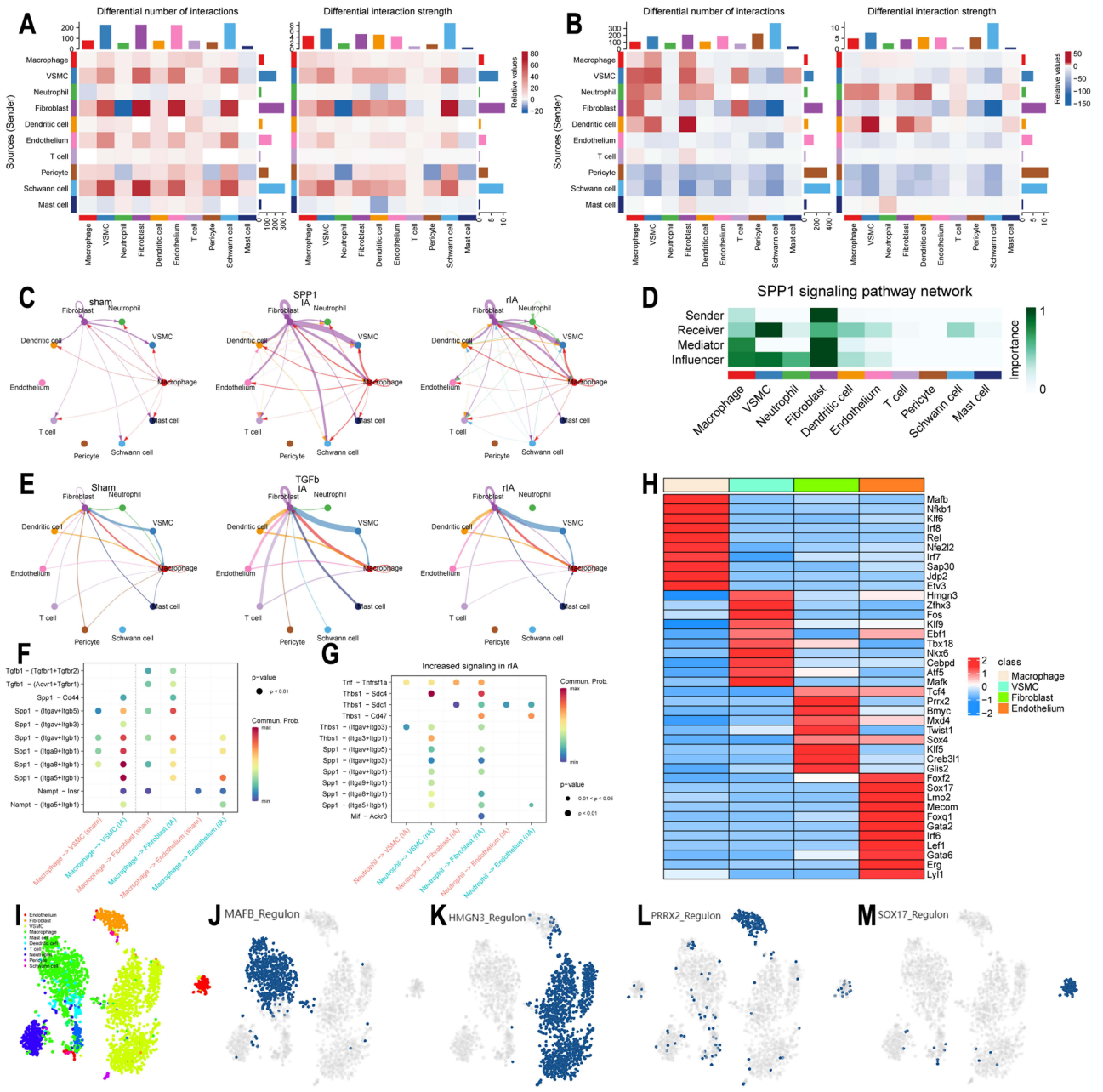

Figure 3 Overall summary of modulatory mechanisms in sham, IA, and rIA groups. (**A**) Heatmap of intercellular interactions between sham and IA groups. (**B**) Heatmap of intercellular interactions between IA and rIA groups. (**C**) Circular plot of SPP1 pathway in 3 groups. (**D**) Heatmap of SPP1 pathway in 10 cell populations. (**E**) Circular plot of TGF-β pathway in 3 groups. (**F**) Bubble plot of L-R pairs in SPP1 pathway originating from macrophages and targeting VSMCs, fibroblasts, endothelial cells between sham and IA groups. (**G**) Bubble plot of increased L-R pairs in the SPP1 pathway originating from neutrophils and targeting VSMCs, fibroblasts, and endothelial cells between the IA and rIA groups. (**H**) Heatmap of top 10 TF regulons in macrophages, VSMCs, fibroblasts, and endothelia. (**I**) t-SNE plot of 10 cell populations. (**J–M**) t-SNE plot of MAFB, HMGN3, PRRX2, SOX17 regulons in macrophages, VSMCs, fibroblasts, and endothelia, respectively.

IL1b, was considered a proinflammatory macrophage responsible for the formation and rupture of IA. Enrichment and pathway scores revealed that the NF-κB, TNF, and TLR pathways were remarkably enhanced (Figure 4C). The M2 subpopulation highly expressed GAS6. Lysosome and endocytosis pathways were also enriched in GAS6^{+} Macrophage. IL1b^{+} Macrophage was increased in IA and rIA, whereas GAS6^{+} Macrophage showed the opposite trend and was most abundant in the sham group (Figure 4B). Interestingly, SPP1^{+} M3 subpopulation significantly increased with the pathogenesis of IA, especially rIA (Figure 4B and F). Compared with GAS6^{+} Macrophage, SPP1^{+} Macrophage was significantly increased in rIA tissue with elevated oxidative phosphorylation. Therefore, the role of SPP1^{+} Macrophage was further discussed.

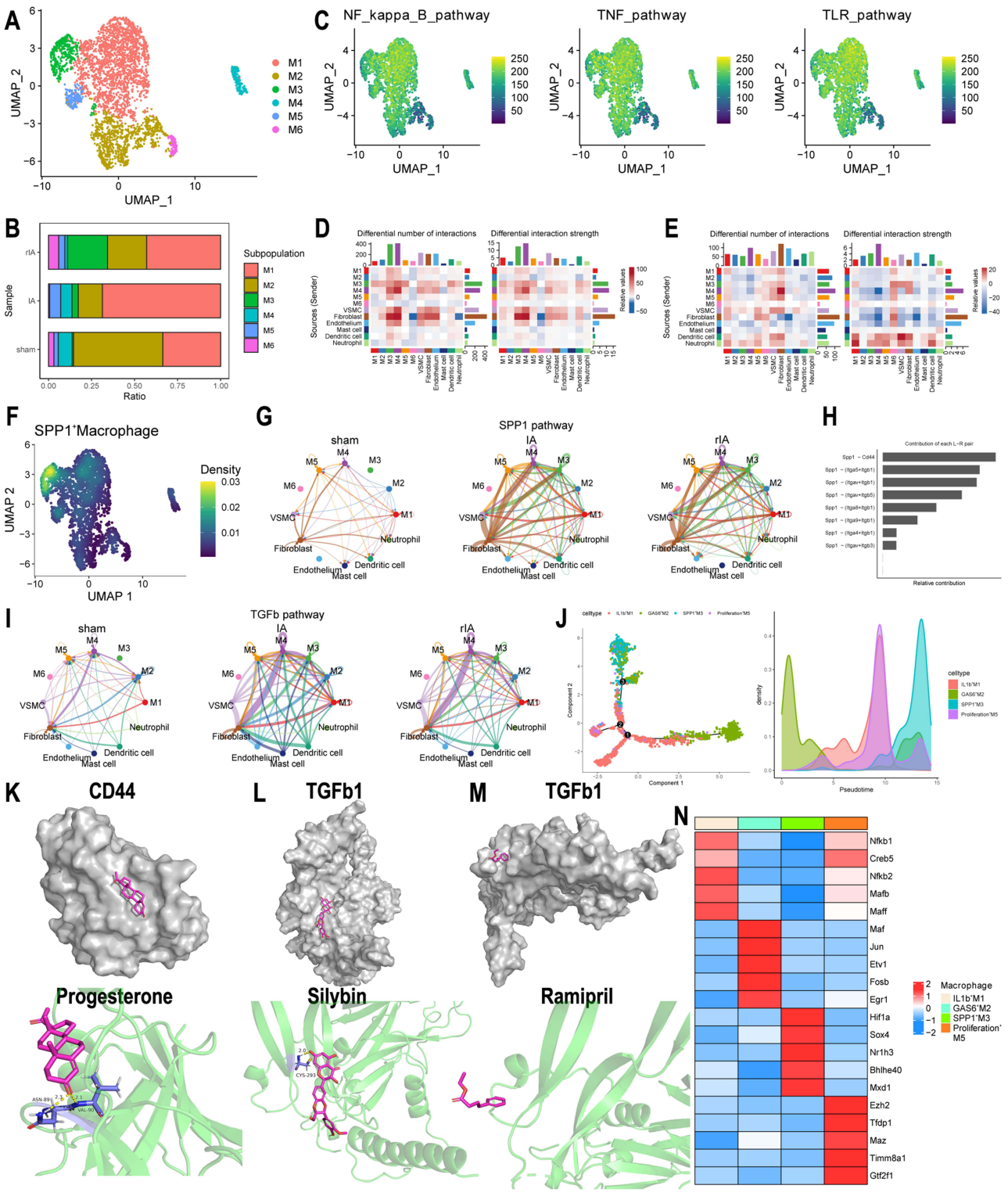

Figure 4 The roles of SPP1$^+$ Macrophage in sham, IA, and rIA groups. (**A**) UMAP plots of 5 macrophage subpopulations. (**B**) Proportions of 5 macrophage subpopulations in three groups. (**C**) Gene set scores of NF-κB pathway, TNF pathway, and TLR pathway. (**D**) Intercellular interactions between sham and IA groups. (**E**) Intercellular interactions between IA and rIA groups. (**F**) UMAP plot of SPP1$^+$ Macrophage in IA. (**G**) Circular plot of SPP1 pathway in 3 groups. (**H**) The composition of L-R pairs in SPP1 pathway. (**I**) Circular plot of TGF-β pathway in 3 groups. (**J**) Differentiation state of IL1b$^+$ Macrophage, GAS6$^+$ Macrophage, SPP1$^+$ Macrophage, and proliferation$^+$ Macrophage based on Pseudotime analysis. (**K–M**) Molecular docking of CD44-Progesterone, TGF-β1-Silybin, and TGF-β1-Ramipril, respectively. (**N**) Heatmap of top 5 TF regulons in IL1b$^+$ Macrophage, GAS6$^+$ Macrophage, SPP1$^+$ Macrophage, and proliferation$^+$ Macrophage.

Intercellular communication analysis revealed that SPP1$^+$ Macrophage mainly interacted with fibroblasts and VSMCs in IA, which might be regulated by neutrophils in rIA (Figure 4D, E, and G). Our results also revealed that SPP1$^+$ Macrophage might promote IA pathogenesis through TGF-β pathway (Figure 4I). The SPP1-CD44 was the L-R pair with the largest proportion in SPP1 pathway, which might be inhibited by progesterone to exert protective effects (Figure 4H and K).[24] Based on molecular docking, silybin and ramipril were also identified as potential drugs for IA and rIA, respectively (Figure 4L and M).[25,26] Then, the M4, M5, and M6 subpopulations were defined as VSMCs, proliferation$^+$ Macrophage, and B cells. Based on pseudotime analysis, SPP1$^+$ Macrophage gradually differentiated and developed from GAS6$^+$ and proliferation$^+$ Macrophage (Figure 4J). Hypoxia-inducible factor 1a (HIF1α) and BHLHE40 regulons were enriched in SPP1$^+$ Macrophage to modulate the progression of IA (Figure 4N).[27] In addition, the corresponding TF regulons that regulated macrophages polarization were observed in IL1b$^+$ and GAS6$^+$ Macrophage (Figure 4N).

The Causality of Collagen Families and Cardiovascular Risk Factors with IA and SAH

Our results revealed that collagen matrix remodeling was involved in the formation and rupture of IA, and the causal relationship between collagen families and IA was further explored. However, no significant associations were observed (Figure 5A and B). Interestingly, systolic blood pressure, diastolic blood pressure, and pulse pressure increased the risk of IA and SAH, suggesting the importance of favorable blood pressure management (Figure 5C and D).[28,29] Similar to single-cell sequencing and clinical cohorts, MR also suggested that neutrophils increased the risk of IA and SAH by 1.29 and 1.17 folds respectively (Figure 5E and F).

Key Cis-pQTLs for IA and SAH Based on Proteome-Wide MR

Due to the absence of single-cell sequencing data for IA, we analyzed three AAA mouse models constructed using Angiotensin II, calcium chloride, and elastase, all of which showed that SPP1$^+$ Macrophage was significantly increased in AAA (Figure 6A and B, Supplementary Figure 2A and B). Next, the effects of SPP1$^+$ Macrophage on IA and SAH were further examined using MR. After removing linkage disequilibrium, we obtained exposure factors associated with IA or SAH from 2998 cis-pQTLs of 1538 proteins. For patients with IA, 39 risk-related and protective proteins were obtained, all of which passed the Steiger Direction Test and Steiger Filtering (Figure 6C). Enrichment analysis revealed that they were mainly involved in the toll-like receptor and pattern recognition receptor pathways, which were also

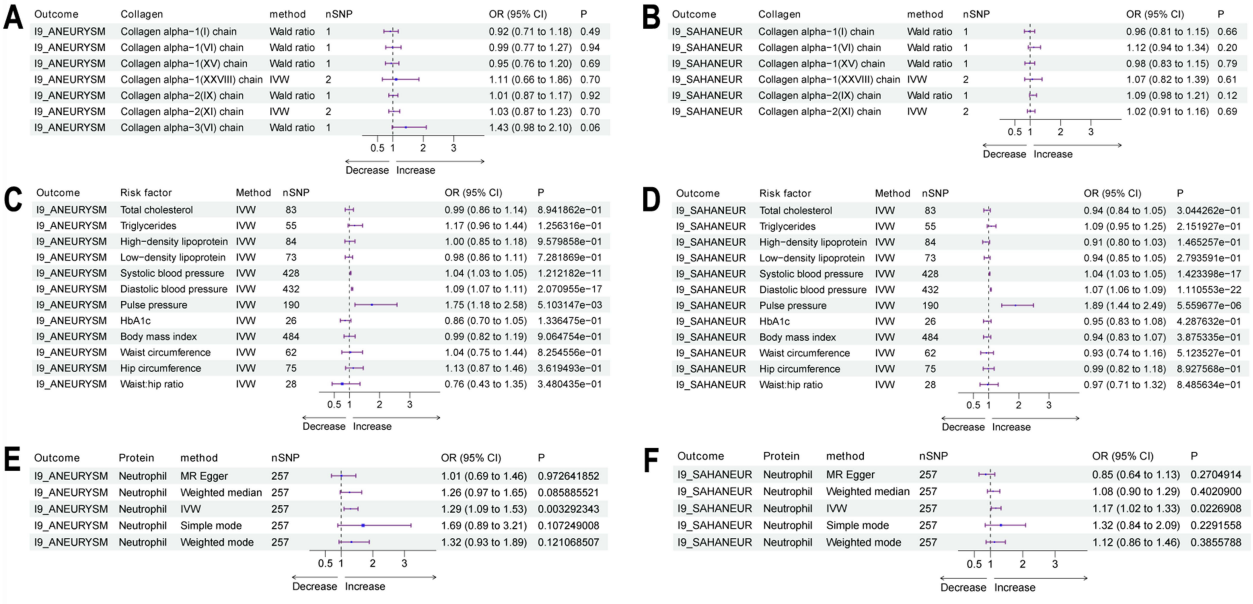

Figure 5 The causality of risk factors in IA and SAH based on Mendelian randomization. (**A** and **B**) The causality of collagen families in patients with IA and SAH. (**C** and **D**) The causality of 12 cardiovascular risk factors in patients with IA and SAH. (**E** and **F**) The causality of Neutrophil number in patients with IA and SAH.

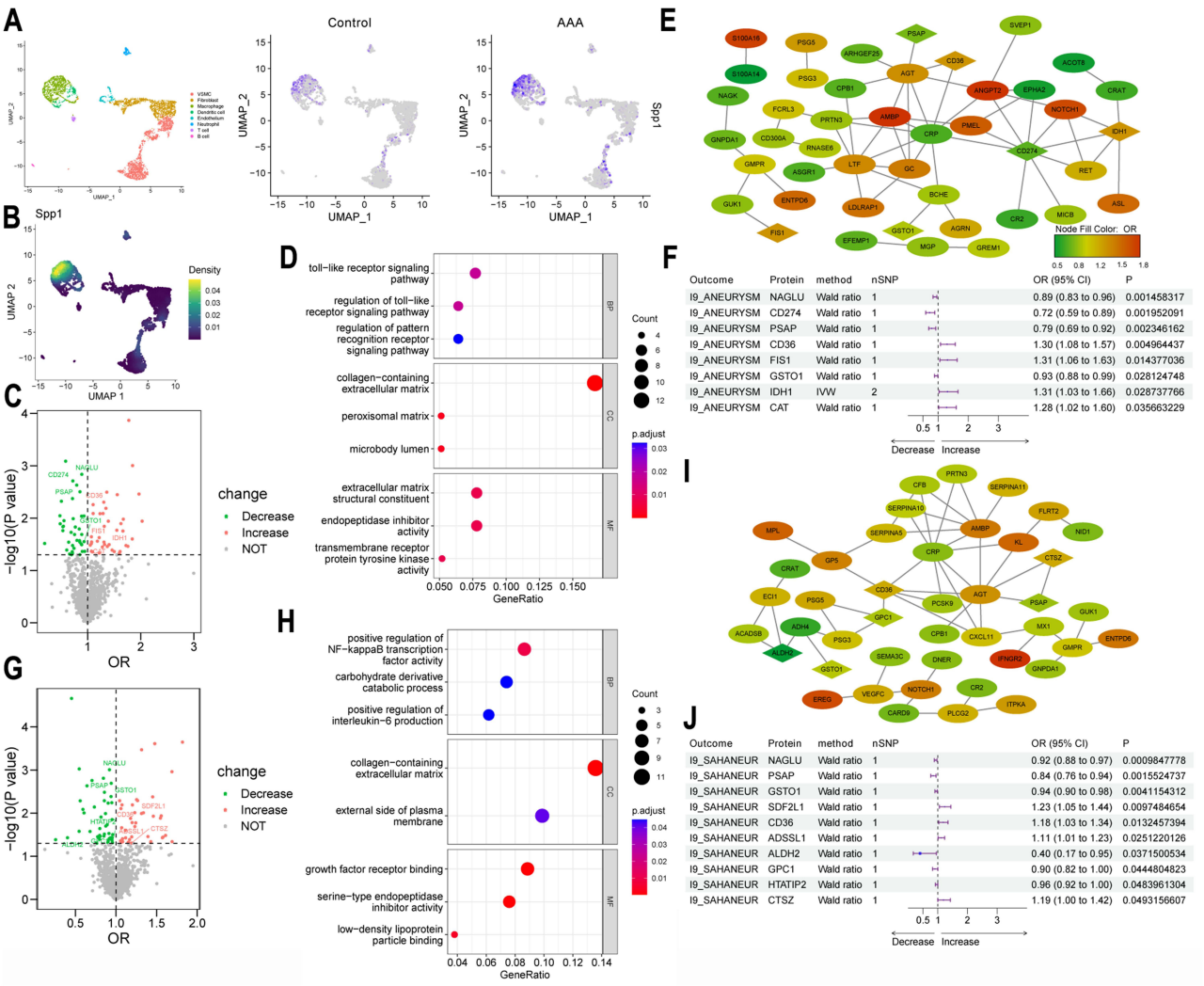

Figure 6 The roles of cis-pQTLs related to SPP1$^+$ Macrophage in IA and SAH. (**A** and **B**) UMAP plot of SPP1$^+$ Macrophage in $CaCl_2$-induced AAA. (**C**) Volcano plot of cis-pQTLs related to IA, labeled as specifically expressed genes in SPP1$^+$ Macrophage. (**D**) Enrichment analysis of cis-pQTLs related to IA. (**E**) PPI network of cis-pQTLs related to IA. (**F**) The causality of cis-pQTLs corresponding to the specifically expressed genes of SPP1$^+$ Macrophage in IA. (**G**) Volcano plot of cis-pQTLs related to SAH, labeled as specifically expressed genes in SPP1$^+$ Macrophage. (**H**) Enrichment analysis of cis-pQTLs related to SAH. (**I**) PPI network of cis-pQTLs related to SAH. (**J**) The causality of cis-pQTLs corresponding to the specifically expressed genes of SPP1$^+$ Macrophage in SAH.

involved in ECM remodeling (Figure 6D). Among these, 4 risk proteins (CD36, FIS1, IDH1, and CAT) and 4 protective proteins (NAGLU, CD274, PSAP, and GSTO1) were highly expressed in SPP1$^+$ Macrophage (Figure 6C and F). A PPI network was constructed to explore these interactions (Figure 6E). Similarly, 40 risk proteins and 45 protective proteins were identified in patients with SAH (Figure 6G). They mainly participated in inflammation-associated pathways, including NF-kB and IL-6 (Figure 6H). Eventually, 4 risk proteins (SDF2L1, CD36, ADSSL1, and CTSZ) and 6 protective proteins (NAGLU, PSAP, GSTO1, ALDH2, GPC1, and HTATIP2) were enriched in SPP1$^+$ Macrophage (Figure 6G and J). These interactions were further visualized in the PPI network (Figure 6I).

Key Cis-eQTLs for IA and SAH Based on Transcriptome-Wide MR

To identify the underlying mechanisms, 955 cis-eQTLs of 432 specifically expressed genes in SPP1$^+$ Macrophage were obtained to complete MR. Among these, 17 risk genes and 15 protective genes for IA were identified ($p < 0.05$) (Figure 7A). 9 risk genes and 20 protective genes for SAH were identified ($p < 0.05$) (Figure 7B). For IA and SAH, only PSAP exerted protective effects at both the gene and protein levels, whereas NAGLU exerted opposite effects. The remaining cis-pQTLs, corresponding to the genes mentioned above, were not statistically significant.

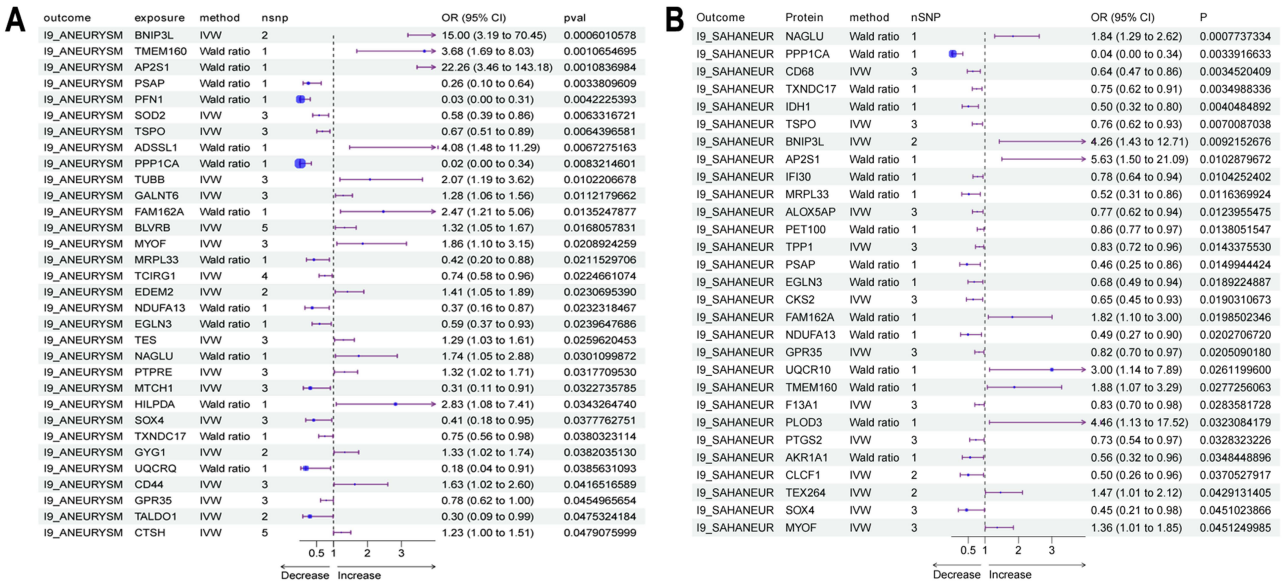

Figure 7 The roles of cis-eQTLs related to SPP1$^+$ Macrophage in IA and SAH. (**A**) The causality of cis-eQTLs corresponding to the specifically expressed genes of SPP1$^+$ Macrophage in IA. (**B**) The causality of cis-eQTLs corresponding to the specifically expressed genes of SPP1$^+$ Macrophage in SAH.

Transcriptome Sequencing Analysis and Immune Infiltration Analysis

After removing the batch effect, there were 469 upregulated and 458 downregulated DEGs between 30 controls and 33 IA patients (Figure 8A). Enrichment analysis revealed that the collagen matrix, vascular smooth muscle, and inflammation-associated pathways were enriched (Figure 8C and D). Moreover, in the 33 IA and 24 rIA patients, 186 upregulated and 210 downregulated DEGs were identified, respectively (Figure 8B). Among these, inflammation-associated pathways were enriched in the rIA group (Supplementary Figure 3A and B). Macrophages accounted for the largest proportion of IA, and the infiltration of activated mast cells also increased (Figure 8E). Although there was no obvious difference in macrophages between IA and rIA, they were still the most abundant cell type (Supplementary Figure 3C). The combined analysis of single-cell and transcriptome sequencing also indicated that macrophages gradually increased with IA progression (Figure 8F). We further screened two hub PPI modules with scores of 35.333 and 10.125 containing 40 and 31 genes, respectively (Figure 8G and H). KEGG enrichment analysis revealed that inflammation- and ECM-associated pathways were enriched in cluster 1 and 2 (Supplementary Figure 3D and E). Interestingly, SPP1 was identified in the interaction center of cluster 2 and its expression increased with the progression of IA, possibly indicating its role in collagen matrix remodeling (Figure 8H and I). However, MR results revealed that the SPP1 polymorphism was not a risk factor for IA or SAH (Supplementary Figure 3F).

WGCNA and Identify Diagnostic Biomarkers

The modules with a correlation coefficient ≥ 0.55 were considered to be significantly associated with IA, which included 1121 genes. Similarly, there were 1440 genes were screened as being associated with rIA (Figure 9A). After combining the results from WGCNA, DEG, and genes corresponding to cis-pQTLs or cis-eQTLs, we identified CD36 and EDEM2 as diagnostic biomarkers for IA and rIA, respectively (Figure 9B). In tissues, the AUC value of EDEM2 for IA was 0.983, while those of CD36 for IA and rIA were 0.746 and 0.751, respectively (Figure 9C). Moreover, the expression of EDEM2 in tissues gradually increased with IA progression (Figure 9D). In the blood, CD36 was highly effective in the early detection of SAH, with an AUC value of 0.997 (Figure 9E). However, its diagnostic value for IA remained unsatisfactory. In rIA and SAH, CD36 was highly expressed in tissue, whereas the opposite phenomenon was observed in the blood (Figure 9F). Regardless, there was no denying its significant diagnostic value in patients with SAH.

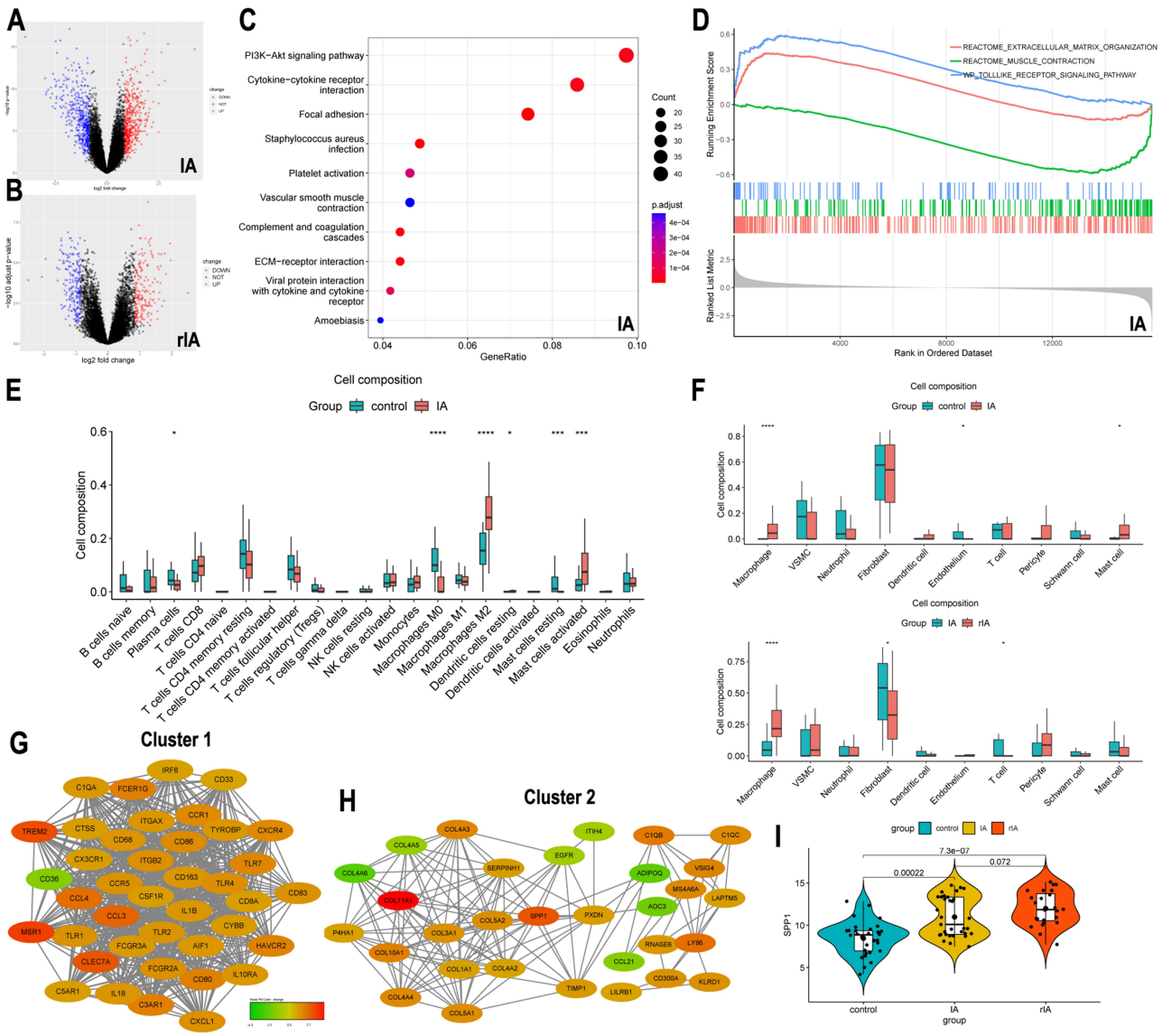

Figure 8 Transcriptome sequencing data among control, IA, and rIA groups. (**A**) Volcano plot of DEGs between the control and IA groups. (**B**) Volcano plot of DEGs between the IA and rIA groups. (**C** and **D**) KEGG and GSEA enrichment analyses between the control and IA groups. (**E**) Immune infiltration analysis between the control and IA groups using CIBERSORT. (**F**) Composition of 10 cell populations based on single-cell and transcriptome sequencing data among the control, IA, and rIA groups. (**G** and **H**) Two PPI modules based on DEGs between the control and IA groups. (**I**) Violin plot of SPP1 using transcriptome sequencing data among the control, IA, and rIA groups. *p < 0.05, ***p < 0.001, ****p < 0.0001.

Clinical Characteristics and Diagnostic Model of IA and SAH

Single-cell sequencing and MR demonstrated that neutrophil infiltration was increased in rIA and was a risk factor for IA and SAH. We further constructed a retrospective clinical cohort, including 281 normal, 282 IA, and 133 SAH participants, to identify the roles of neutrophils and related indicators. Interestingly, female patients with high blood pressure were more likely to develop IA, which was associated with an increased risk of SAH (Table 1). Immune cells in the blood changed significantly in SAH but not in IA. Both univariate and multivariate regression analyses revealed that female sex and hypertension were risk factors for IA (Table 2, Figure 10A). Hypertension (OR [95% CI] = 4.49 [3.00,6.82]; p = 2 × 10^(−13)) was the most important risk factor. Immune cells, including leukocytes, neutrophils, and monocytes, were significantly increased in SAH. Similar results were observed for neutrophil-related indicators, including the PNR, NLR, and SII (Table 1). However, significant multicollinearity was observed among the variables in the multivariate regression analysis of SAH. The RF machine-learning algorithm was used to identify important risk factors

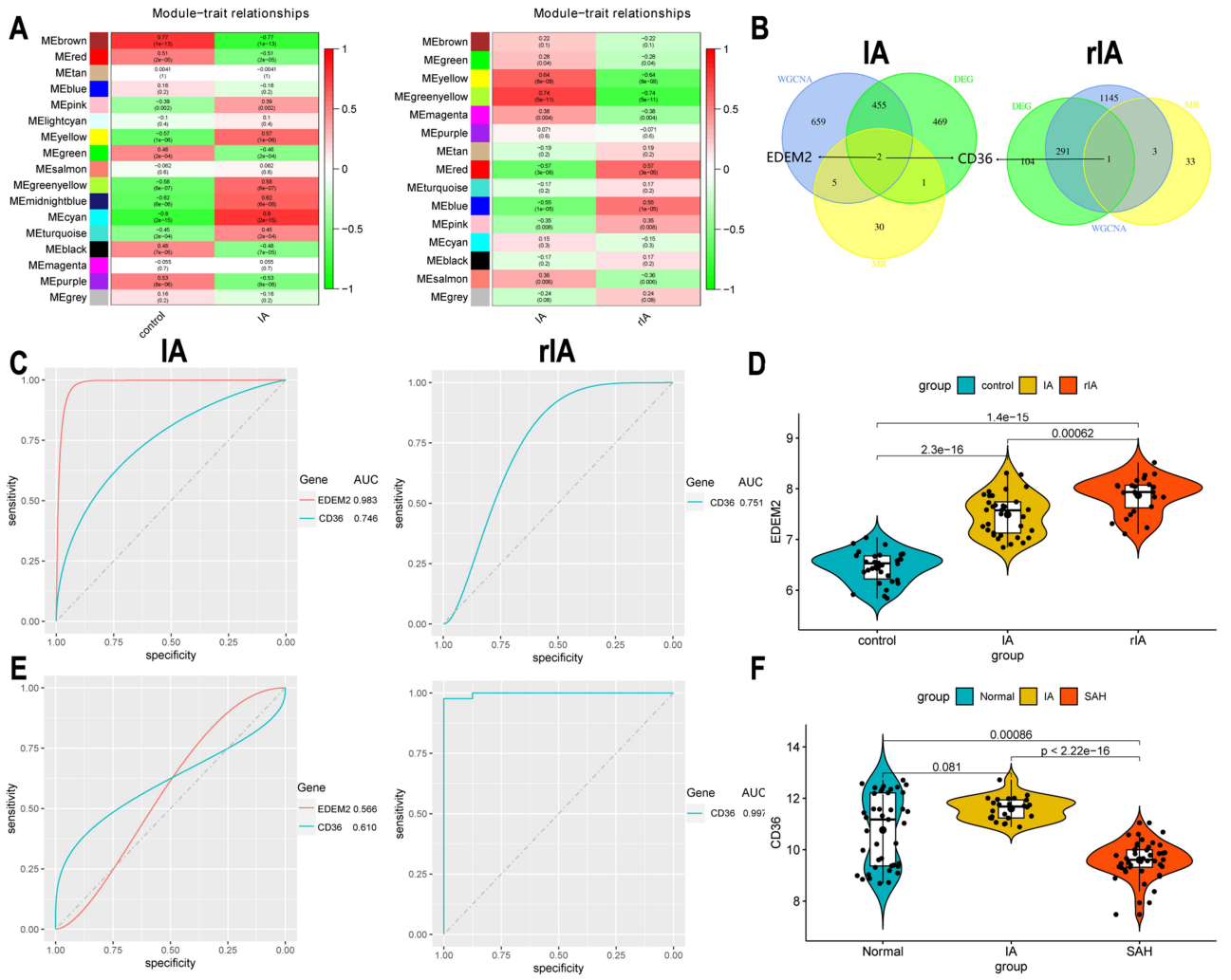

Figure 9 Diagnostic biomarkers of IA and rIA derived from SPP1$^+$ Macrophage and transcriptome sequencing data. (**A**) Heatmap of associations between gene modules and IA, rIA, respectively. (**B**) Venn plot of common genes in WGCNA modules, DEG, and SPP1$^+$ Macrophage in IA and rIA. (**C**) ROC curves for diagnostic biomarkers of IA and rIA in tissues. (**D**) Expression of EDEM2 among control, IA, and rIA in tissues. (**E**) ROC curves for diagnostic biomarkers of IA and rIA in blood. (**F**) Expression of CD36 among control, IA, and rIA in blood.

based on the 11 variables in the univariate regression analysis. Similar to the above results, NLR and neutrophil count were the two most important risk factors for SAH (Figure 10B). The proportions of neutrophils and macrophages were significantly upregulated in the rIA tissue. These cells were possibly derived from the blood and promoted the rupture of IA. Eventually, the top 7 risk factors were included in the risk score for SAH diagnosis, with an AUC value of 0.981, which could be beneficial for the management of SAH caused by IA rupture (Figure 10C).

Table 1 Clinical Variables of Control, IA, and SAH Participants

Variable	Con N=281	IA N=288	SAH N=135	Con VS IA P value	IA VS SAH P value	ALL P value
Age	61.09±38.00	58.23±10.36	59.79±25.95	1	1	0.419
Sex						
Male	164(58.36%)	85(29.51%)	42(31.11%)	<0.001	0.853	<0.001
Female	117(41.64%)	203(70.49%)	93(68.89%)			

(*Continued*)

Table 1 (Continued).

Variable	Con N=281	IA N=288	SAH N=135	Con VS IA P value	IA VS SAH P value	ALL P value
Hypertension						
Yes	72(25.62%)	157(54.51%)	70(51.85%)	<0.001	0.684	<0.001
No	209(74.38%)	131(45.49%)	65(48.15%)			
Diabetes						
Yes	33(11.74%)	29(10.07%)	8(5.93%)	0.613	0.222	0.178
No	248(88.26%)	259(89.93%)	127(94.07%)			
Examination						
Leukocyte, 10^9/L	5.74±1.33	5.56±1.45	10.37±3.31	0.819	<0.001	<0.001
RBC, 10^{12}/L	4.47±0.43	4.43±0.45	4.30±0.49	0.648	0.01	<0.001
HB, g/L	136.59±12.94	131.86±16.09	128.82±16.76	<0.001	0.324	<0.001
PLT, 10^9/L	229.19±53.37	234.22±61.51	217.22±74.17	1	0.024	0.023
Lymphocyte, 10^9/L	1.87±0.53	1.73±0.54	1.16±0.93	0.004	<0.001	<0.001
Monocyte, 10^9/L	0.39±0.12	0.36±0.12	0.45±0.21	0.004	<0.001	<0.001
Neutrophil, 10^9/L	3.29±1.04	3.39±1.14	8.66±3.22	1	<0.001	<0.001
PNR	78.23±52.13	76.59±33.41	28.36±14.83	1	<0.001	<0.001
NLR	1.88±0.80	2.14±1.21	10.35±7.41	0.007	<0.001	<0.001
PLR	129.8±38.68	146.79±59.12	236.13±118.46	<0.001	<0.001	<0.001
PWR	41.33±11.23	43.71±14.17	22.34±8.72	0.197	<0.001	<0.001
SII	427.88±192.75	499±304.61	2177.68±1678.97	0.008	<0.001	<0.001

Table 2 Univariate Logistic Regression Analysis of Variables in Control, IA, and SAH Participants

Variable	Univariate-IA		Univariate-SAH	
	OR (95% CI)	P	OR (95% CI)	P
Age	0.99 (0.98 to 1.00)	0.314	1.01 (0.99 to 1.02)	0.404
Male	0.30 (0.21 to 0.42)	<0.001	1.08 (0.69 to 1.68)	0.738
Hypertension	3.48 (2.45 to 4.98)	<0.001	0.90 (0.60 to 1.35)	0.609
Diabetes	0.84 (0.49 to 1.43)	0.522	0.56 (0.23 to 1.21)	0.164
Examination				
Leukocyte, 10^9/L	0.95 (0.84 to 1.07)	0.372	2.92 (2.39 to 3.67)	<0.001
RBC, 10^{12}/L	0.82 (0.56 to 1.19)	0.289	0.54 (0.34 to 0.85)	0.008
HB, g/L	0.98 (0.97 to 0.99)	<0.001	0.99 (0.98 to 1.00)	0.076
PLT, 10^9/L	1.00 (1.00 to 1.00)	0.298	1.00 (0.99 to 1.00)	0.015

(*Continued*)

Table 2 (Continued).

Variable	Univariate-IA		Univariate-SAH	
	OR (95% CI)	P	OR (95% CI)	P
Lymphocyte, 10^9/L	0.62 (0.45 to 0.84)	0.003	0.15 (0.09 to 0.23)	<0.001
Monocyte, 10^9/L	0.11 (0.03 to 0.44)	0.002	46.90 (11.48 to 207.17)	<0.001
Neutrophil, 10^9/L	1.08 (0.93 to 1.26)	0.296	4.18 (3.19 to 5.79)	<0.001
PNR	1.00 (1.00 to 1.00)	0.655	0.88 (0.86 to 0.90)	<0.001
NLR	1.33 (1.10 to 1.64)	0.005	2.83 (2.29 to 3.63)	<0.001
PLR	1.01 (1.00 to 1.01)	<0.001	1.01 (1.01 to 1.02)	<0.001
PWR	1.01 (1.00 to 1.03)	0.028	0.83 (0.79 to 0.86)	<0.001
SII	1.00 (1.00 to 1.00)	0.002	1.00 (1.00 to 1.00)	<0.001

Discussion

There were no obvious symptoms of unruptured IA, except for nerve compression, which was commonly ignored by patients and went undiagnosed. However, SAH caused by rIA was typically accompanied by severe neurological dysfunction, which had devastating consequences. In our study, $SPP1^+$ Macrophage has been recognized to promote collagen matrix remodeling and phenotypic transformation. These cells could regulate VSMCs and fibroblasts via the SPP1/CD44 pair. Then cis-pQTLs and cis-eQTLs corresponding to genes in $SPP1^+$ Macrophage were analyzed to uncover the pathogenesis of IA and SAH. Combining GWAS and transcriptome sequencing data, CD36 emerged as a shared risk factor for both IA and SAH, which was further considered as an efficient diagnostic biomarker for SAH in blood. Meanwhile, blood pressure and peripheral neutrophil count were considered risk factors for patients with IA and SAH using MR analysis, which was further demonstrated in our retrospective cohort study. Neutrophils and related indicators were identified as diagnostic biomarkers for early SAH detection. This study aimed to provide novel insights into the diagnosis and therapy of IA and rIA from multi-omics and clinical transformation perspectives.

Single-cell sequencing analysis revealed that macrophage infiltration increased with IA progression in our study, indicating its important roles. Among them, $IL1b^+$ Macrophage is present in the aortas of atherosclerotic mice and promote plaque formation,[30] whereas $GAS6^+$ Macrophage is recognized to maintain homeostasis mediated by efferocytosis, playing a protective role in IA.[31] In our study, $SPP1^+$ Macrophage gradually increased with IA progression, especially in rIA. The number of $SPP1^+$ Macrophage also increased in AAA models induced by Angiotensin II, calcium chloride, and elastase. A recent study has demonstrated that $SPP1^+$ Macrophage induced by type 3 inflammation causes collagen IV degradation and collagen I deposition, which promotes lung and liver fibrosis through TGF-β1.[32] $SPP1^+$

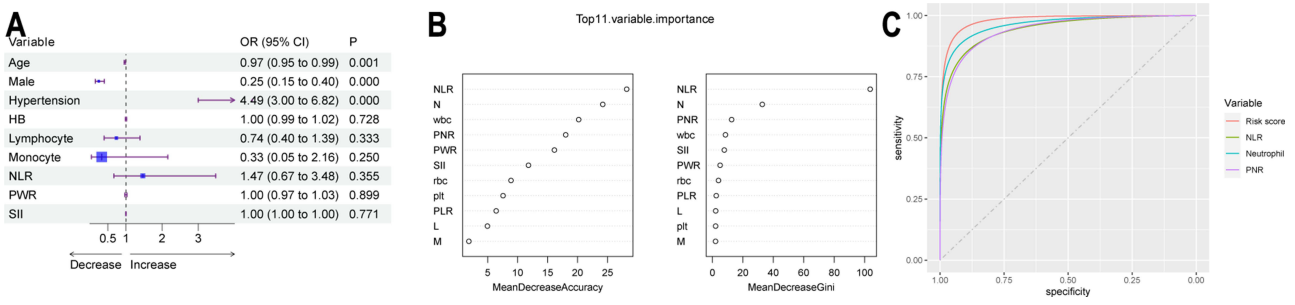

Figure 10 Clinical variables and diagnostic biomarkers among control, IA, and SAH participants. (**A**) Multivariate logistic regression analysis of clinical variables in IA participants. (**B**) Ranking of the top 11 variables in SAH participants based on RF algorithm. (**C**) ROC curves of risk score and neutrophil-related indicators in the blood of SAH patients.

Macrophage is also increased in idiopathic pulmonary fibrosis, further activating fibroblasts to accelerate fibrosis.[33] In TAA, SPP1 derived from fibroblasts not only reduces the expression of contractile genes ACTA2 and TAGLN in VSMCs, but also increases collagen expression in fibroblasts.[34] SPP1 is also demonstrated to promote the development of AAA and increase in blood, suggesting that it could be secreted into circulation and affect systemic vessels, which probably provides novel insights for therapeutic target.[35] Our study revealed that SPP1 was highly expressed in VSMCs and fibroblasts, which have the ability to synthesize the extracellular matrix. Based on SCENIC analysis, it was demonstrated that the HIF1α and BHLHE40 regulons specifically regulate $SPP1^+$ Macrophage. In the acute stage of autoimmune myocarditis, HIF1α mediates immune overactivation in macrophages and T-helper cells, worsening the cardiac function.[36] A recent study has demonstrated that metabolic reprogramming of macrophages activated HIF1α, whose target genes induce vascular inflammation and ECM remodeling, causing the progression of aortic dissection.[27] BHLHE40 maintains the migration function of macrophage and exerts widespread proinflammatory effects by increasing the expression of HIF1α, which also participates in metabolic reprogramming by promoting glycolysis.[37] Interestingly, a previous study has demonstrated that SPP1 could regulate the expression of HIF1α.[38] Therefore, we propose that $SPP1^+$ Macrophage not only regulates the phenotypic transformation of VSMC and ECM remodeling through SPP1 and TGF-β pathways but also mediates inflammation and metabolic reprogramming through HIF1α, ultimately causing the formation and rupture of IA.

Enrichment analysis of cis-pQTLs in $SPP1^+$ Macrophage revealed that inflammation and ECM remodeling-associated pathways were enriched in both IA and rIA, indicating that protein polymorphisms regulated the progression of aneurysm by altering their original function. The roles of $SPP1^+$ Macrophage in IA and SAH were further explored from the perspective of MR. Among them, the CD36 rs6961069 polymorphism proposed in this study was a common risk factor for IA and SAH, providing novel insights for early prevention. CD36 is a pattern recognition receptor and fatty acid transporter that promotes inflammation and regulates cellular metabolism in various types of cells. It could take up oxidized low-density lipoprotein to promote oxidative stress and foam cell formation, thus exert pro-atherosclerotic effects. Recent studies have also demonstrated that the polymorphisms in CD36 are significantly associated with dyslipidemia, lipid oxidation, and coronary heart disease.[39,40] Regular administration of statins is an independent predictor of aneurysm wall enhancement in unruptured fusiform IA, which is also negatively correlated with SAH.[41,42] Therefore, we have reason to believe that CD36 could serve as an effective therapeutic target for IA and SAH, with the added advantage of being easily applied in clinical practice. NAGLU rs77942990 and PSAP rs2394843 were common protective factors for IA and SAH. NAGLU is a lysosomal enzyme mainly involved in the degradation of mucopolysaccharides. The relationship between NAGLU and aneurysms is unclear, but its deficiency increases inflammation, collagen deposition, and fibrosis in myocardial tissue.[43] Similarly, PSAP is a precursor protein of several lysosomal enzymes that could increase the efferocytosis efficiency of macrophages and exert anti-inflammatory effects.[44] Another study has demonstrated that PSAP improves neuronal activity and reduces infarct size in mice with middle cerebral artery occlusion by inhibiting apoptosis.[45] Although ALDH2 is considered to reduce oxidative stress to protect cardiomyocytes, the polymorphism of ALDH2 rs671 reduces its enzyme activity, thereby decreasing the risk of developing AAA by nearly 50%. Specifically, the inhibition of ALDH2 improves the phenotypic transformation of VSMCs by interacting with the myocardium, which is partially associated with miR-31-5p.[46,47] It is worth noting that ALDH2 rs671 is primarily found in East Asian populations, while ALDH2 rs570600621, as identified in this study, is a risk factor for SAH and is more prevalent in European populations.

Our results revealed that neutrophils were a risk factor for IA and SAH, and their related indicators were highly effective in diagnosing patients with SAH. In an acute aortic dissection (AAD) model induced by Ang II, CXCL1 and G-CSF are predominantly increased in circulation to induce neutrophil infiltration in tissues, causing interleukin 6 release to promote AAD rupture.[48] Consistent with our cohort, neutrophils and NLR are predominantly increased in the peripheral blood of SAH patients, which might become useful biomarkers to evaluate IA instability.[49] In AAA patients undergoing emergency surgery, an elevated NLR was significantly associated with higher in-hospital mortality and postoperative multiple organ failure.[50] A recent study revealed that multiple systemic inflammation indicators were correlated with arrhythmia, including atrial fibrillation, ventricular arrhythmia, and bradyarrhythmia, based on a 478,544 UK Biobank cohort.[51] Neutrophils and related indicators serve as convenient and rapid peripheral blood biomarkers and

are helpful for early identification of patients with SAH. In our study, CD36 was also considered an effective diagnostic biomarker for patients with SAH, particularly in blood samples. However, there are still a limited number of studies on the associations between CD36 and patients with SAH. Although the diagnostic biomarkers proposed in our study hold significant value for identifying patients with SAH, further validation in large clinical cohorts is still required.

Conclusion

$SPP1^+$ Macrophage was consistently increased in several aneurysms, thus promoting pathological phenotype transformation and ECM remodeling through the SPP1 and TGF-β pathways. Based on cis-pQTLs and cis-eQTLs related to $SPP1^+$ Macrophage, CD36 was both a risk factor for IA and SAH and an efficient diagnostic biomarker for SAH in blood. Moreover, neutrophils and related indicators have also been considered excellent diagnostic biomarkers of SAH in a clinical cohort.

Data Sharing Statement

Single-cell and transcriptome sequencing datasets were obtained from the GEO database. The GWAS data was derived from the IEU database. Any data not mentioned in our paper and supplementary materials can be acquired from the corresponding author under reasonable conditions.

Acknowledgments

We would like to thank the GEO and IEU databases utilized in the study for their valuable data in scientific research.

Author Contributions

All authors made a significant contribution to the work reported, whether that is in the conception, study design, execution, acquisition of data, analysis and interpretation, or in all these areas; took part in drafting, revising or critically reviewing the article; gave final approval of the version to be published; have agreed on the journal to which the article has been submitted; and agree to be accountable for all aspects of the work.

Funding

This work was supported by the National Natural Science Foundation of China [Nos. 81601721, 82070382 and 82371574], the Natural Science Foundation of Shandong Province [Nos. ZR2023MH306 and ZR2023MH026], and Taishan Scholars Program [No. ts 20190979].

Disclosure

The authors declare that this research is conducted in the absence of any commercial or financial relationships that could be construed as potential conflicts of interest.

References

1. Etminan N, Rinkel GJ. Unruptured intracranial aneurysms: development, rupture and preventive management. *Nat Rev Neurol*. 2016;12(12):699–713.
2. Brown RD Jr, Broderick JP. Unruptured intracranial aneurysms: epidemiology, natural history, management options, and familial screening. *Lancet Neurol*. 2014;13(4):393–404.
3. Frösen J, Cebral J, Robertson AM, Aoki T. Flow-induced, inflammation-mediated arterial wall remodeling in the formation and progression of intracranial aneurysms. *Neurosurg Focus*. 2019;47(1):E21.
4. Chalouhi N, Hoh BL, Hasan D. Review of cerebral aneurysm formation, growth, and rupture. *Stroke*. 2013;44(12):3613–3622. doi:10.1161/STROKEAHA.113.002390
5. Etminan N, Dörfler A, Steinmetz H. Unruptured intracranial aneurysms- pathogenesis and individualized management. *Deutsches Arzteblatt Int*. 2020;117(14):235–242. doi:10.3238/arztebl.2020.0235
6. Jiang B, Paff M, Colby GP, Coon AL, Lin LM. Cerebral aneurysm treatment: modern neurovascular techniques. *Stroke Vasc Neurol*. 2016;1(3):93–100. doi:10.1136/svn-2016-000027
7. Sawyer DM, Pace LA, Pascale CL, et al. Lymphocytes influence intracranial aneurysm formation and rupture: role of extracellular matrix remodeling and phenotypic modulation of vascular smooth muscle cells. *J Neuroinflammation*. 2016;13(1):185. doi:10.1186/s12974-016-0654-z
8. Doran S, Arif M, Lam S, et al. Multi-omics approaches for revealing the complexity of cardiovascular disease. *Briefings Bioinf*. 2021;22(5):bbab061. doi:10.1093/bib/bbab061

9. Sanchez S, Chimenti MS, Lu Y, et al. Modulation of the immunological milieu in acute aneurysmal subarachnoid hemorrhage: the potential role of monocytes through CXCL10 secretion. *Translational Stroke Res*. 2024. doi:10.1007/s12975-024-01259-4
10. Moraes L, Grille S, Morelli P, et al. Immune cells subpopulations in cerebrospinal fluid and peripheral blood of patients with aneurysmal subarachnoid hemorrhage. *SpringerPlus*. 2015;4:195. doi:10.1186/s40064-015-0970-2
11. Wang X, Zhang A, Yu Q, et al. Single-cell RNA sequencing and spatial transcriptomics reveal pathogenesis of meningeal lymphatic dysfunction after experimental subarachnoid hemorrhage. *Adv Sci*. 2023;10(21):e2301428. doi:10.1002/advs.202301428
12. Molenberg R, Thio CHL, Aalbers MW, et al. Sex hormones and risk of aneurysmal subarachnoid hemorrhage: a Mendelian randomization study. *Stroke*. 2022;53(9):2870–2875. doi:10.1161/STROKEAHA.121.038035
13. Pietzner M, Wheeler E, Carrasco-Zanini J, et al. Mapping the proteo-genomic convergence of human diseases. *Science*. 2021;374(6569):eabj1541.
14. Sun Z, Yun Z, Lin J, et al. Comprehensive mendelian randomization analysis of plasma proteomics to identify new therapeutic targets for the treatment of coronary heart disease and myocardial infarction. *J Transl Med*. 2024;22(1):404. doi:10.1186/s12967-024-05178-8
15. Lin PW, Lin ZR, Wang WW, Guo AS, Chen YX. Identification of immune-inflammation targets for intracranial aneurysms: a multiomics and epigenome-wide study integrating summary-data-based mendelian randomization, single-cell-type expression analysis, and DNA methylation regulation. *Int j Surg*. 2024. doi:10.1097/JS9.0000000000001990
16. He Q, Wang W, Xiong Y, et al. Causal association between circulating inflammatory cytokines and intracranial aneurysm and subarachnoid hemorrhage. *Eur J Neurol*. 2024;31(8):e16326.
17. Vlachogiannis P, Hillered L, Enblad P. Ronne-Engström E Elevated levels of several chemokines in the cerebrospinal fluid of patients with subarachnoid hemorrhage are associated with worse clinical outcome. *PLoS One*. 2023;18(3):e0282424. doi:10.1371/journal.pone.0282424
18. Chaudhry SR, Kinfe TM, Lamprecht A, et al. Elevated level of cerebrospinal fluid and systemic chemokine CCL5 is a predictive biomarker of clinical outcome after aneurysmal subarachnoid hemorrhage (aSAH). *Cytokine*. 2020;133:155142. doi:10.1016/j.cyto.2020.155142
19. Kim HK, Lee KO, Oh SH, et al. The clinical significance of peripheral blood cell ratios in patients with intracranial aneurysm. *Front Neurol*. 2022;13:1080244. doi:10.3389/fneur.2022.1080244
20. Wang RH, Wen WX, Jiang ZP, et al. The clinical value of neutrophil-to-lymphocyte ratio (NLR), systemic immune-inflammation index (SII), platelet-to-lymphocyte ratio (PLR) and systemic inflammation response index (SIRI) for predicting the occurrence and severity of pneumonia in patients with intracerebral hemorrhage. *Front Immunol*. 2023;14:1115031. doi:10.3389/fimmu.2023.1115031
21. Martinez AN, Tortelote GG, Pascale CL, et al. Single-cell transcriptome analysis of the circle of Willis in a mouse cerebral aneurysm model. *Stroke*. 2022;53(8):2647–2657. doi:10.1161/STROKEAHA.122.038776
22. Hu C, Li T, Xu Y, et al. CellMarker 2.0: an updated database of manually curated cell markers in human/mouse and web tools based on scRNA-seq data. *Nucleic Acids Res*. 2023;51(D1):D870–d876. doi:10.1093/nar/gkac947
23. Vanneste D, Bai Q, Hasan S, et al. MafB-restricted local monocyte proliferation precedes lung interstitial macrophage differentiation. *Nat Immunol*. 2023;24(5):827–840.
24. Ohlsson C, Langenskiöld M, Smidfelt K, et al. Low progesterone and low estradiol levels associate with abdominal aortic aneurysms in men. *J Clin Endocrinol Metab*. 2022;107(4):e1413–e1425. doi:10.1210/clinem/dgab867
25. Yang Q, Tan T, He Q, et al. Combined amphiphilic silybin meglumine nanosuspension effective against hepatic fibrosis in mice model. *Int J Nanomed*. 2023;18:5197–5211. doi:10.2147/IJN.S407762
26. Tan WQ, Fang QQ, Shen XZ, et al. Angiotensin-converting enzyme inhibitor works as a scar formation inhibitor by down-regulating Smad and TGF-β-activated kinase 1 (TAK1) pathways in mice. *Br J Pharmacol*. 2018;175(22):4239–4252. doi:10.1111/bph.14489
27. Lian G, Li X, Zhang L, et al. Macrophage metabolic reprogramming aggravates aortic dissection through the HIF1α-ADAM17 pathway(□). *EBioMedicine*. 2019;49:291–304.
28. Kristensen KE, Torp-Pedersen C, Gislason GH, et al. Angiotensin-converting enzyme inhibitors and angiotensin II receptor blockers in patients with abdominal aortic aneurysms: nation-wide cohort study. *Arteriosclerosis Thrombosis Vasc Biol*. 2015;35(3):733–740. doi:10.1161/ATVBAHA.114.304428
29. Chen SW, Chan YH, Lin CP, et al. Association of long-term use of antihypertensive medications with late outcomes among patients with aortic dissection. *JAMA network open*. 2021;4(3):e210469. doi:10.1001/jamanetworkopen.2021.0469
30. Cochain C, Vafadarnejad E, Arampatzi P, et al. Single-cell RNA-seq reveals the transcriptional landscape and heterogeneity of aortic macrophages in murine atherosclerosis. *Circulation Res*. 2018;122(12):1661–1674. doi:10.1161/CIRCRESAHA.117.312509
31. Nepal S, Tiruppathi C, Tsukasaki Y, et al. STAT6 induces expression of Gas6 in macrophages to clear apoptotic neutrophils and resolve inflammation. *Proc Natl Acad Sci USA*. 2019;116(33):16513–16518. doi:10.1073/pnas.1821601116
32. Fabre T, Barron AMS, Christensen SM, et al. Identification of a broadly fibrogenic macrophage subset induced by type 3 inflammation. *Science Immunol*. 2023;8(82):eadd8945. doi:10.1126/sciimmunol.add8945
33. Morse C, Tabib T, Sembrat J, et al. Proliferating SPP1/MERTK-expressing macrophages in idiopathic pulmonary fibrosis. *Europ Resp J*. 2019;54:2. doi:10.1183/13993003.02441-2018
34. Zhou M, Zhu Y, Zhou Z, et al. Fibroblast-secreted phosphoprotein 1 mediates extracellular matrix deposition and inhibits smooth muscle cell contractility in Marfan syndrome aortic aneurysm. *J Cardiovasc Transl Res*. 2022;15(5):959–970. doi:10.1007/s12265-022-10239-8
35. Wang SK, Green LA, Gutwein AR, et al. Osteopontin may be a driver of abdominal aortic aneurysm formation. *J Vascular Surg*. 2018;68(6s):22s–29s. doi:10.1016/j.jvs.2017.10.068
36. Hua X, Hu G, Hu Q, et al. Single-cell RNA sequencing to dissect the immunological network of autoimmune myocarditis. *Circulation*. 2020;142(4):384–400.
37. Zafar A, Ng HP, Kim GD, Chan ER. Mahabeleshwar G H BHLHE40 promotes macrophage pro-inflammatory gene expression and functions. *FASEB J*. 2021;35(10):e21940. doi:10.1096/fj.202100944R
38. Tu W, Zheng H, Li L, et al. Secreted phosphoprotein 1 promotes angiogenesis of glioblastoma through upregulating PSMA expression via transcription factor HIF1α. *Acta Biochim Biophys Sin*. 2022;55(3):417–425. doi:10.3724/abbs.2022157
39. Chen Y, Zhang J, Cui W, Silverstein RL. CD36, a signaling receptor and fatty acid transporter that regulates immune cell metabolism and fate. *J Exp Med*. 2022;219:6. doi:10.1084/jem.20211314
40. Shu H, Peng Y, Hang W, et al. The role of CD36 in cardiovascular disease. *Cardiovascular Res*. 2022;118(1):115–129. doi:10.1093/cvr/cvaa319

41. Peng F, Niu H, Feng X, et al. Aneurysm wall enhancement, atherosclerotic proteins, and aneurysm size may be related in unruptured intracranial fusiform aneurysms. *Eur Radiol*. 2023;33(7):4918–4926. doi:10.1007/s00330-023-09456-9
42. Yoshimura Y, Murakami Y, Saitoh M, et al. Statin use and risk of cerebral aneurysm rupture: a hospital-based case-control study in Japan. *J Stroke Cerebrovascular Dis*. 2014;23(2):343–348. doi:10.1016/j.jstrokecerebrovasdis.2013.04.022
43. Schiattarella GG, Cerulo G, De Pasquale V, et al. The murine model of mucopolysaccharidosis iiib develops cardiopathies over time leading to heart failure. *PLoS One*. 2015;10(7):e0131662. doi:10.1371/journal.pone.0131662
44. Bhattacharya P, Dhawan UK, Hussain MT, et al. Efferocytes release extracellular vesicles to resolve inflammation and tissue injury via prosaposin-GPR37 signaling. *Cell Rep*. 2023;42(7):112808. doi:10.1016/j.celrep.2023.112808
45. Yu J, Li J, Matei N, et al. Intranasal administration of recombinant prosaposin attenuates neuronal apoptosis through GPR37/PI3K/Akt/ASK1 pathway in MCAO rats. *Exp Neurol*. 2024;373:114656. doi:10.1016/j.expneurol.2023.114656
46. Yang K, Ren J, Li X, et al. Prevention of aortic dissection and aneurysm via an ALDH2-mediated switch in vascular smooth muscle cell phenotype. *Eur Heart J*. 2020;41(26):2442–2453. doi:10.1093/eurheartj/ehaa352
47. Zhang J, Guo Y, Zhao X, et al. The role of aldehyde dehydrogenase 2 in cardiovascular disease. *Nat Rev Cardiol*. 2023;20(7):495–509. doi:10.1038/s41569-023-00839-5
48. Anzai A, Shimoda M, Endo J, et al. Adventitial CXCL1/G-CSF expression in response to acute aortic dissection triggers local neutrophil recruitment and activation leading to aortic rupture. *Circulation Res*. 2015;116(4):612–623. doi:10.1161/CIRCRESAHA.116.304918
49. Wu XB, Zhong JL, Wang SW, et al. Neutrophil-to-lymphocyte ratio is associated with circumferential wall enhancement of unruptured intracranial aneurysm. *Front Neurol*. 2022;13:879882. doi:10.3389/fneur.2022.879882
50. Garagoli F, Fiorini N, Pérez MN, et al. Neutrophil-to-lymphocyte ratio and platelet-to-lymphocyte ratio predict in-hospital mortality in symptomatic but unruptured abdominal aortic aneurysm patients. *Int Angiology*. 2022;41(3):188–195. doi:10.23736/S0392-9590.22.04754-X
51. Yang X, Zhao S, Wang S, et al. Systemic inflammation indicators and risk of incident arrhythmias in 478,524 individuals: evidence from the UK Biobank cohort. *BMC Med*. 2023;21(1):76. doi:10.1186/s12916-023-02770-5